

# PROCESS OPTIMIZATION OF CHITOSAN STABILIZED ZEROVALENT IRON NANOPARTICLE SYNTHESIS USING RESPONSE SURFACE METHODOLOGY

<sup>1</sup>P.Prema, <sup>2</sup>S.M. Nitin Bala

<sup>1</sup>Assistant Professor, Research Department of Zoology, V.H.N.Senthikumara Nadar College, Virudhunagar-626001, Tamil Nadu, India.

<sup>2</sup>Department of Chemical Engineering, Amrita Vishwa Vidyapeetham, Amritanagar, Ettimadai, Coimbatore-641112, Tamil Nadu, India.

**Abstract:** In the present research pursuit, synthesis of chitosan stabilized zerovalent iron nanoparticles (CH-Fe<sup>0</sup>) through green synthesis method using chitosan as stabilizing agent. The optimum conditions for synthesis of chitosan stabilized iron nanoparticles were analysed using Response surface methodology (RSM) based central composite design (CCD) using Design Expert software (7.0.0 trial version). The synthesized particles were characterized by Zetasizer, Fourier transform infrared spectroscopy (FT-IR), x-ray diffractogram (XRD), scanning electron microscopy (SEM), energy dispersive spectroscopy (EDS) and atomic force microscopy (AFM) to analyze size, morphology and quantitative informations respectively. Four experimental parameters were chosen as independent variables: concentration of FeSO<sub>4</sub> (molar), volume of reducing agent KBH<sub>4</sub> (ml), N<sub>2</sub> gas purging time (minutes) and chitosan (%) as stabilizing agent. A quadratic model was established as a functional relationship between four independent variables and the effective hydrodynamic diameter (nm) of chitosan stabilized zerovalent iron nanoparticles. The results of model fitting and statistical analysis demonstrated that only chitosan concentration was statistically significant parameter.

**Keywords:** polymer synthesis, chitosan iron nanoparticles, zeta sizer, central composite design, characterization

## 1. INTRODUCTION

Nanotechnology is expected to revolutionize both science and modern civilization. Nanotechnology involves puddle work at atomic levels, tweaking and controlling substances 1, 00, 000 times smaller than a strand of human hair, to make useful materials and devices. It involves technology at the scale of one-billionth of a meter. In recent years, the field of nanoscience and nanotechnology is one of the most popular areas for current research and development in basically all technical disciplines. In the last two decades, nanotechnology is considered to be one of the most important advancements in science and technology. At nano scale materials exhibit unique properties that can be used for novel applications like magnetization. Nanoscale iron particles have large surface areas and high surface reactivity (Zhang 2003). Biopolymers have been used to stabilize the zerovalent iron nanoparticles which resulted in more effective nanocomposites, such as water-soluble starch (He and Zhao 2005), chitosan and its derivatives (Adewuyi et al 2012; Akinremi et al 2013). Chitosan is one of the most abundant natural polymers, nontoxic, biodegradable and biocompatible. Chitosan has high reactivity and processability for its specific molecular structure and polycationic nature.

Design of experiments (DOE) and response surface methodology (RSM) is largely used for modeling mechanism parameters. It is suitable factorial design and searches the common connection between various factors for the determination of most favorable or unfavorable conditions of the processes. Response surface methodology has different model types such as central composite design (CCD), Doehlert matrix (DM) and Box-Behnken design (BBD). In order to determine the optimum experimental conditions, as well as the effect of various operational parameters, including concentration of FeSO<sub>4</sub>, volume of reducing agent KBH<sub>4</sub>, N<sub>2</sub> gas purging time (minutes) and chitosan in % (stabilizing agent), RSM followed with CCD was applied. By selecting the RSM as an effective statistical and mathematical approach, in order to recognize the efficiency of an experimental system, various parameters were simultaneously appraised with a minimum number of experiments. The present study focuses on applying statistical optimization technique like response surface methodology to optimize the process parameters like concentration of FeSO<sub>4</sub> (molar), volume of reducing agent KBH<sub>4</sub> (ml), N<sub>2</sub> gas purging time (minutes) and chitosan (%) as stabilizing agent by designing the experiments through central composite design (CCD) to improve the yield of synthesis process.

## 2. EXPERIMENTAL

### 2.1. Chemicals and solvents

Ferrous sulfate heptahydrate ( $\text{FeSO}_4 \cdot 7\text{H}_2\text{O}$ ), Potassium borohydride ( $\text{KBH}_4$ ), Chitosan, Nitric acid ( $\text{HNO}_3$ ) and Ethanol ( $\text{C}_2\text{H}_5\text{OH}$ ) were purchased from Himedia (P) Ltd, Mumbai were used as starting materials without further purification. Milli-Q water was used for the synthesis of chitosan stabilized zerovalent iron nanoparticle and also for the preparation of all other aqueous solutions throughout the experiment.

### 2.2. Statistical optimization of chitosan stabilized iron nanoparticle by Central composite design

Response surface methodology is a kind of experimental design methods. A collection of mathematical and statistical techniques helpful for the modeling and analysis of problems in which a response of favorite is influenced by several variables and the objective is to optimize this response is defined as response surface methodology (RSM). The main idea of RSM is to use a sequence of designed experiments to obtain an optimal response. If the fitted surface is a sufficient approximation of the true response function, then analysis of the fitted surface will be nearly equivalent to analysis of the real system. Central composite design (CCD) represents a good choice among the standard designs used in RSM, because of its high efficiency with respect to the number of required runs. CCD is to augment a full factorial design by adding so-called star points (set points) and some number of replicates measurements at the center (center points). By spacing all the points at an equal distance from the center, a rotatable design is obtained that gives each point equal leverage in the estimation of the regression coefficients. In this study, a total of 30 runs were experimentally conducted for the process parameters  $\text{FeSO}_4$  (precursor) concentration (molar),  $\text{KBH}_4$  (reducing agent) in ml,  $\text{N}_2$  gas (min.) and chitosan (%) as stabilizing agent. The process parameters in different ranges and their coded values are presented in Table 1.

**Table 1: Ranges and levels of the independent variables**

Symbol	Independent variable	Coded levels		
		Low (-1)	Center (0)	High (+1)
A	$\text{FeSO}_4$ (Molar concentration)	0.05	0.1	0.15
B	Volume of $\text{KBH}_4$ (ml)	1	3	5
C	$\text{N}_2$ gas (min)	15	30	45
D	Chitosan (%)	0.25	0.5	0.75

In this four factor design, a total of 30 experimental runs were executed and their observations were fitted to the following second order polynomial model:

$$Y = \beta_0 + \beta_1A + \beta_2B + \beta_3C + \beta_4D + \beta_{11}A^2 + \beta_{22}B^2 + \beta_{33}C^2 + \beta_{44}D^2 + \beta_{12}AB + \beta_{12}AC + \beta_{12}AD + \beta_{12}BC + \beta_{12}BD + \beta_{12}CD$$

Where,

Y is the dependent variable (size of Ch- $\text{Fe}^0$  nanoparticle), A, B, C, and D are the independent variables,  $\beta_0$  is the regression coefficient at center points,  $\beta_1$ ,  $\beta_2$ ,  $\beta_3$  and  $\beta_4$  are the linear coefficient;  $\beta_{11}$ ,  $\beta_{22}$ ,  $\beta_{33}$  and  $\beta_{44}$  are the quadratic coefficients. The developed model was evaluated using statistical analysis including analysis of variance (ANOVA) and Fisher's test (F value). The quality of fit of the model equation was expressed by the coefficient of determination,  $R^2$ . The fitted model was then plotted in the form of 3D surface plots in order to illustrate the relationship between responses.

### 2.3. Synthesis of chitosan stabilized $\text{Fe}^0$ nanoparticles (CH- $\text{Fe}^0$ )

CH- $\text{Fe}^0$  nanoparticles were synthesized by reducing  $\text{FeSO}_4 \cdot 7\text{H}_2\text{O}$  with  $\text{KBH}_4$  in the presence of chitosan as a stabilizer (Geng et al 2009b). Chitosan (0.5% w/v) was dissolved in 0.05 M  $\text{HNO}_3$ . Due to the poor solubility of chitosan, the mixture was stirred overnight and filtered through 0.22  $\mu\text{m}$  syringe filters to remove any suspensions. Then, 10 mL of solution containing 0.2978 g of  $\text{FeSO}_4 \cdot 7\text{H}_2\text{O}$  was mixed with 3 mL of 0.5% chitosan solution. The mixture was stirred for 30 minutes under  $\text{N}_2$  gas, and then 5 mL of freshly prepared aqueous solution of  $\text{KBH}_4$  (0.3467g) was added drop wise. The obtained black particles were separated from the solution by centrifugation at 4000 rpm for 5 minutes and washed twice with  $\text{N}_2$  gas saturated Milli-Q water and at least three times with 99% absolute ethanol. Finally, the synthesized Ch- $\text{Fe}^0$  nanoparticles were dried in an oven at 60°C and used for further studies.

### 2.4. Characterization of Zerovalent Iron Nanoparticles

All glasswares used in the present experiment were washed well using nitric acid and rinsed with deionized water followed by Milli Q water for prior to use. The reduction of metal ions was roughly monitored by visual inspection of color change in the reaction solution. Powder form synthesized chitosan stabilized zerovalent iron nanoparticles were mixed with KBr to obtain KBr pellets consisting of 1.5% (w/w) of the nanoparticles. The resulting mixture was pressed into disks (0.5 mm in thickness). FTIR spectrum was achieved in a Shimadzu FT-IR spectrophotometer and registering amplitude waves ranging from 550-4000  $\text{cm}^{-1}$ . Diffraction patterns of all the nanoparticles were examined using a X'Pert Pro Materials Research diffractometer system, with  $\text{CuK}\alpha$  radiation and amplitude wave  $\lambda = 1.5418 \text{ \AA}$  working with a 40 kV voltage and 30 mA current. The resultant diffraction intensities were compared with the standard JCPDS (Joint Committee on Powder Diffraction Standards) files. The morphological characteristics of all the nanoparticles were obtained through scanning electron microscopy (JEOL SU Model 1510) operated at 5 kV, magnification x10 k. Elemental analysis of nanoparticles was carried out using EDS instrument (JSM 35 CF JEOL) in a resolution of 60  $\text{\AA}$ , operated at 15.0 kV with a magnification of 5 k. The size and morphology of the  $\text{Fe}^0$  nanoparticles were examined by atomic force microscope (AFM, SPM-9500J3, Shimadzu Co., Japan). For AFM, nanoparticles suspended in water were placed on a glass slide by dropping 100  $\mu\text{l}$  of the sample, and was allowed to dry for 5 minutes. The slide was then scanned with AFM in non-contact mode. Particle size distribution was carried out by means of dynamic light scattering method using a particle size analyzer (Zeta sizer -SZ-100

nano series, Horiba, Japan). Around 3 ml of the synthesized silver solution was subjected to particle size analysis to determine the hydrodynamic size of the nanoparticles. The measurement of zeta potential is based on the direction and velocity of particles under the influence of known electric field. Zeta potential values of the experimental sample predict the nature of electrostatic potential near the surface of the particles by mixing an aliquot of the sample with  $10^{-3}$ M KCl solution prior to analysis.

Run order	Factor A	Factor B	Factor C	Factor D	Particle size (nm)	Predicted value
1	0.15	5.00	15.00	0.25	96	97.46
2	0.15	5.00	45.00	0.75	112	113.48
3	0.05	5.00	15.00	0.25	98	102.23
4	0.10	3.00	30.00	0.50	48	51.26
5	0.05	1.00	45.00	0.75	108	106.68
6	0.10	3.00	30.00	0.25	94	93.42
7	0.10	1.00	30.00	0.25	92	90.71
8	0.05	1.00	45.00	0.25	64	65.69
9	0.15	5.00	15.00	0.75	114	114.30
10	0.05	5.00	15.00	0.75	106	105.96
11	0.05	1.00	45.00	0.25	98	97.54
12	0.10	3.00	30.00	0.75	112	112.67
13	0.10	3.00	45.00	0.50	46	46.86
14	0.05	5.00	30.00	0.25	92	94.68
15	0.10	3.00	30.00	0.75	114	114.36
16	0.10	3.00	15.00	0.75	68	69.98
17	0.15	1.00	30.00	0.50	104	104.84
18	0.15	3.00	45.00	0.75	96	94.56
19	0.15	1.00	30.00	0.50	72	74.07
20	0.10	3.00	30.00	0.50	46	48.24
21	0.10	3.00	45.00	0.50	44	46.58
22	0.05	5.00	15.00	0.75	114	114.64
23	0.05	1.00	15.00	0.75	96	100.8
24	0.10	3.00	45.00	0.50	78	79.8
25	0.15	1.00	30.00	0.25	98	96.68
26	0.10	3.00	30.00	0.50	48	51.26
27	0.10	3.00	30.00	0.50	48	51.26
28	0.10	3.00	30.00	0.75	124	125.4
29	0.15	5.00	45.00	0.25	84	82.86
30	0.15	1.00	15.00	0.25	108	109.8

**Table 2: The experimental design and the obtained responses**

### 3. RESULTS AND DISCUSSION

#### 3.1. Statistical optimization using central composite design

Based on the response surface methodology result, the optimum conditions of the four significant factors in order to produce smallest sized Ch-Fe<sup>o</sup> nanoparticles. For each run, the experiment along with the predicted particle size obtained from the regression equation for the 30 combinations are shown in Table 2. For predicting the optimal values of Ch-Fe<sup>o</sup> nanoparticle synthesis within the experimental constrains, a second order polynomial model was fitted to the experimental results by design expert software. The model developed was expressed as follows.

$$Y (\text{Ch-Fe}^{\circ} \text{ nanoparticle size, nm}) = 58.84 + 5.88*A - 0.82*B - 7.74*C - 14.26*D - 8.20*A^2 + 17.58*B^2 + 5.07*C^2 + 6.14*D^2 - 7.86*A*B - 1.58*A*C + 0.79*A*D + 2.58*B*C - 0.83*B*D - 2.19*C*D$$

The above mentioned statistical equation indicates that the positive values have a synergistic effect on the response regression model and in this model p-value < 0.001. The F-test value presents how the mean square of the model compares to the mean square of the residuals. The model F test value of 5.15 implies (Ch-Fe<sup>o</sup> nanoparticle size in nm) and the negative values represent an antagonistic effect on the response in the respective factors.

In this equation, the coefficient of one factor presented the effectiveness of this particular factor. To analyze the particle size (yield) through the coefficient values from the equation, it is clear that the chitosan concentration gives a higher positive effect as compared to the other parameters. Values of "Prob > F" was less than 0.05 indicating that the model terms were significant, where a lower probability value represents a higher significance for the that the model is significant and suggesting that there is only a 0.16 % chance for the model F-value to occur due to noise. In this model, linear term D (chitosan, stabilizing agent concentration) and quadratic term D<sup>2</sup> was statistically significant model terms. The lack of fit F value of 0.64 implies the Lack of Fit is not significant relative to the pure error. Non significant lack of fit is good to fit the model (Table 3).

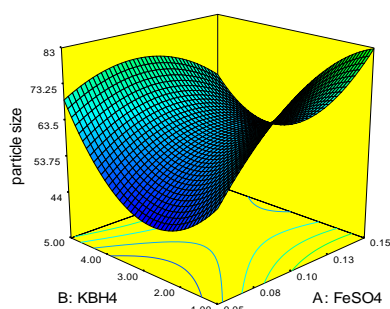
To check the fitness of the model, the coefficient of determination (R<sup>2</sup>) was used. An R<sup>2</sup> value close to 1 implies the better

correlation between experimental and predicted responses. Thus, it is important for a good model  $R^2$  to be within the range of 0-1, and the closer it is to 1, the more fit the model is reported earlier (Reddy et al 2008). In this model, the correlation coefficient ( $R^2$ ) value of 0.8277 is at a reasonable agreement with the adjusted determination coefficient ( $R^2_{Adj}$ ) value of 0.6670 in terms of a high significance of model. The adequate precision measures the signal to noise ratio and values greater than 4 is considered appropriate for the desired model (Fig.1). In the developed model, an adequate precision value of 6.829 for chitosan stabilized nanoparticles size (nm) yield indicates the model can be used to navigate the design space.

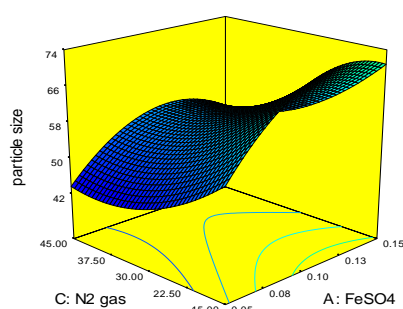
**Table 3: Anova result of the quadratic model**

Source	Degree of freedom	Sum of squares	Mean squares	F-value	P-value	Remarks
Model	14	14913.73	1065.27	5.15	0.0016	significant
A	1	426.06	426.06	2.06	0.1718	
B	1	8.68	8.68	0.042	0.8405	
C	1	777.25	777.25	3.76	0.0717	
D	1	2902.11	2902.11	14.03	0.0019	Significant
AB	1	828.93	4.01	0.0638		
AC	1	39.16	0.19	0.6697		
AD	1	45.49	0.22	0.6459		
BC	1	104.27	0.50	0.4887		
BD	1	46.17	0.22	0.6434		
CD	1	399.02	1.93	0.1852		
A <sup>2</sup>	1	94.72	0.46	0.5089		
B <sup>2</sup>	1	371.06	1.79	0.2004		
C <sup>2</sup>	1	239.81	1.16	0.2987		
D <sup>2</sup>	1	5899.32	28.51	0.0001	0.0001	Significant
Residual	15	3103.13	206.90			
Lack of Fit	8	1306.13	163.27	0.64	0.7308	Not significant
Pure Error	7	1797.33	256.76			
Total	29	18017.20				

$R^2 = 0.827$  Adeq. Precision = 6.829



a



b

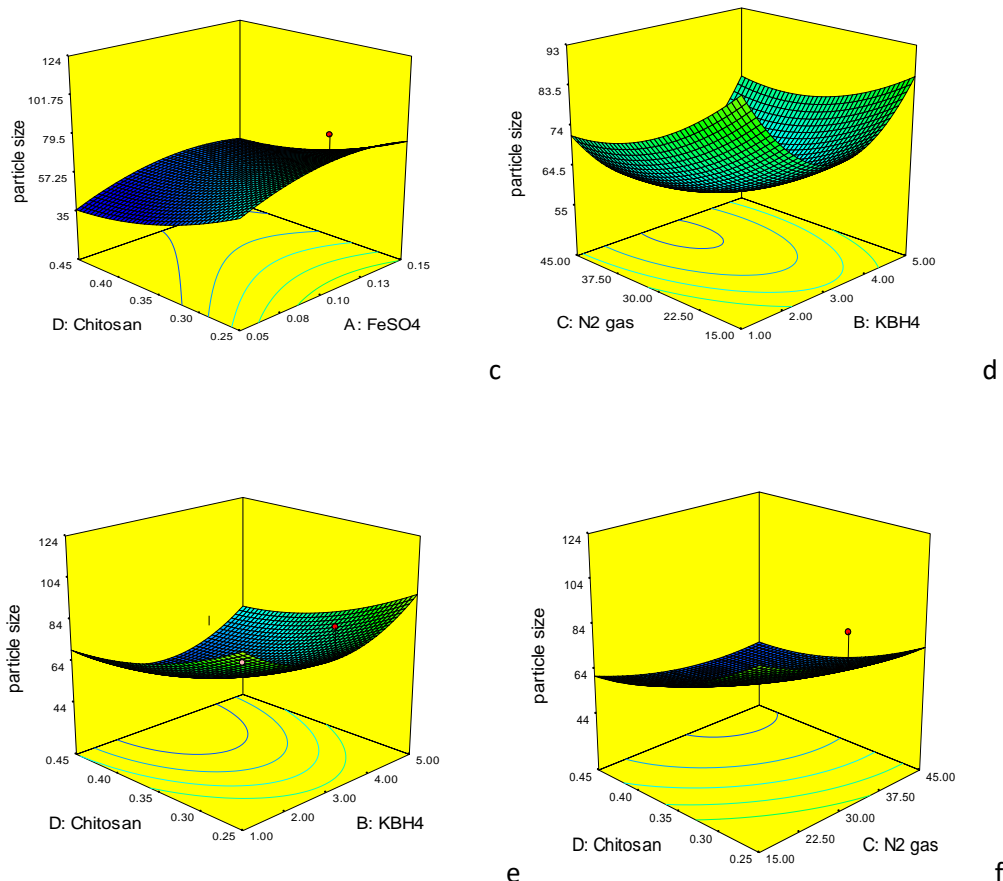


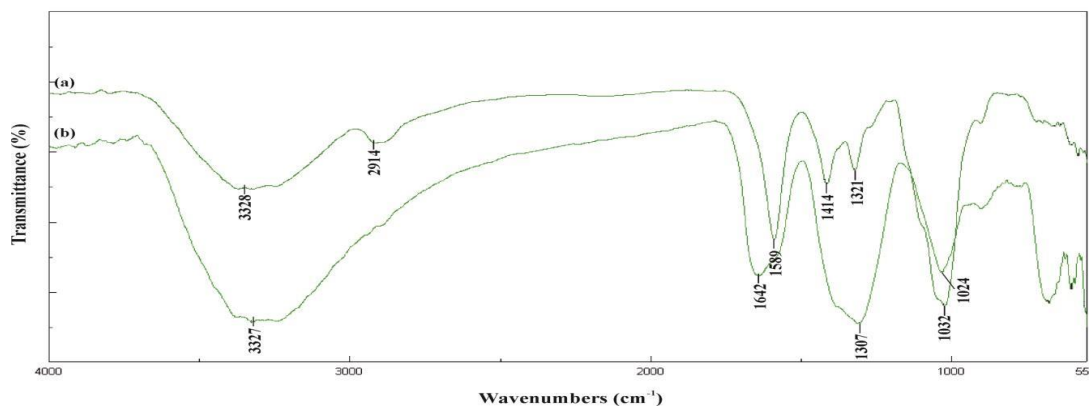
**Fig. 1:** 3D response surface a–f showing the interactive effects of independent variables (FeSO<sub>4</sub>, KBH<sub>4</sub>, N<sub>2</sub> gas and chitosan) on biosynthesis of chitosan stabilized zerovalent iron nanoparticles

### 3.2. Characterization of Fe<sup>0</sup> and CH-Fe<sup>0</sup> nanoparticles

#### 3.2.1. FT-IR Spectroscopy

The main band at 3328 cm<sup>-1</sup> was characteristic of the O-H stretching vibration and the one at 1642 cm<sup>-1</sup> to the O-H bending vibration of surface-adsorbed water. The main bands in the IR spectrum of chitosan are as follows: strong bands at around 3304 cm<sup>-1</sup> (O-H stretch), 1646 cm<sup>-1</sup> and 1375 cm<sup>-1</sup> (amide II), 1035 cm<sup>-1</sup> (skeletal vibration of C-O stretch) and a weak band at 2873 cm<sup>-1</sup> (C-H stretch). The observed data showed several visible changes in the spectrum of CH-Fe<sup>0</sup> in comparison with the spectrum of chitosan (Fig. 2). The stretching bands of the hydroxyl group shifted from 3304 cm<sup>-1</sup> to 3235 cm<sup>-1</sup> for CH-Fe<sup>0</sup> and a clearly measurable decrease (69 cm<sup>-1</sup>) in wave number indicated that O-H vibration was affected due to the iron attachment. On the other hand, the original band of the chitosan component at 1646 cm<sup>-1</sup> for amide II was also shifted to 1641 cm<sup>-1</sup>. These observed results indicated that both hydroxyl (-OH) and amide (-NH<sub>2</sub>) groups of chitosan were mainly involved in the fabrication of iron nanoparticles resulted in the binding of nanoparticles with stabilizer. Based on the FT-IR data, the stabilization of Fe nanoparticles was attributed due to the adsorption of stabilizer molecules onto the surface of the nanoparticles.

If chitosan molecules are adsorbed on the surface of Fe<sup>0</sup> nanoparticles, the stretching frequencies for the functional groups of chitosan are expected to shift significantly (Liang 2007). Earlier studies (Geng et al 2009a) reported that oxygen and nitrogen atoms are the binding sites for chitosan on iron. Similarly, both -OH and -NH<sub>2</sub> groups bonded to the metal ions have been noticed in earlier studies (Bhatia and Ravi 2000 and 2003) and the present results exactly match with these findings.



a-Chitosan b-chitosan stabilized zerovalent iron nanoparticle  
**Fig. 2:** FT-IR spectrum of chitosan stabilized Fe<sup>0</sup> nanoparticles

### 3.2.2. X-Ray Diffraction

The XRD spectrum confirmed that nanoparticles present in the sample was mainly in zerovalent state which was characterized by the basic reflection angle at  $2\theta$  value of  $44.70^\circ - 44.94^\circ$ , the intensive diffraction peaks were observed at  $2\theta$  value of  $44.77^\circ$  was ascribed to the (110) facets of body centered cubic (bcc) Fe (JCPDS File No. 89-7194) unequivocally indicated that the particles were made of pure iron (Fig. 3).

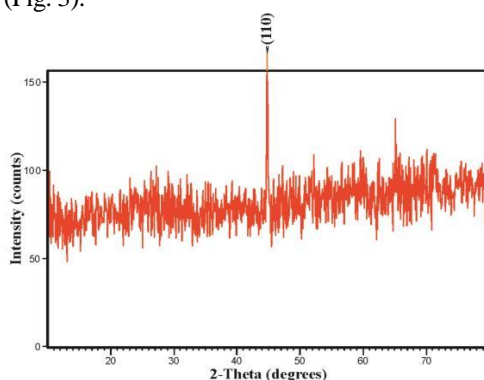


**Fig. 3:** X-ray diffraction spectrum of Ch-Fe<sup>0</sup> nanoparticles

Similarly, the characteristic peak appearing at  $2\theta$  value of  $44.90^\circ$  represent the bcc Fe(0) lattice plane (110) is previously reported (Sun et al 2006; Singhal et al 2012). Earlier researchers (Madhavi et al 2014; Xu et al 2014) examined that the peak at  $2\theta$  value of  $44.70^\circ$  corresponds to (110) reflection plane of iron and the present results corroborate with these reports. The results recorded in the present experiment is in consistent with the XRD pattern obtained earlier (Geng et al 2009a) who reported that a strong peak at  $2\theta = 44.76^\circ$  corresponding to (110) plane indicates the crystalline nature of Fe<sup>0</sup> nanoparticles and in zero valence state.

### 3.2.3. Scanning Electron Microscopy

SEM micrograph of CH-Fe<sup>0</sup> exhibited that the synthesized particles were uniform in size and spherical in shape (Fig. 4). Moreover, SEM image of CH-Fe<sup>0</sup> revealed that the nanoparticles were composed of individual, spherical particles that form aggregates and chains.

The spherical particles aggregated to form dendrites is due to geomagnetic forces and the aggregation of nanoparticles could be attributed to the electrostatic forces between nanoscale particles and their surface tension interactions (Manning et al 2007; Alidokht et al 2011). Earlier reports (Geng et al 2009a) revealed that the presence of chitosan minimize the agglomeration of the resulting iron nanoparticles and thus maintains the high surface area and potential reactivity of the particles.

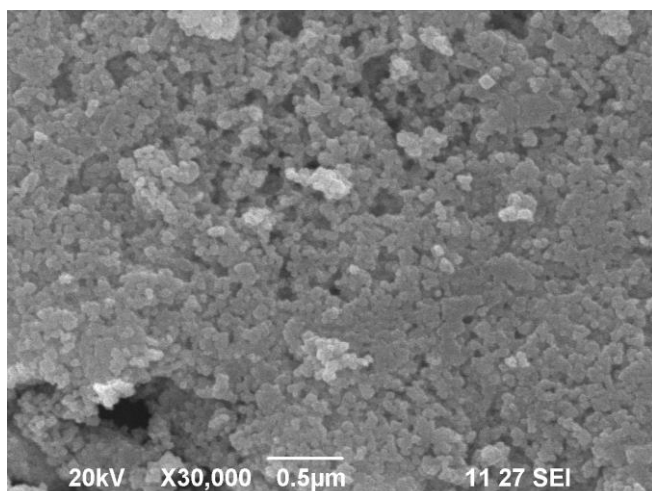


**Fig. 4:** Scanning electron micrograph of Ch-Fe<sup>0</sup> nanoparticles

### 3.2.4. Energy Dispersive Spectroscopy

The EDS spectrum of CH-Fe<sup>0</sup>, a strong peak was obtained at the energy of 6.9 keV for iron (Fig. 5) and also some of the weak peaks for sulfur (S) and oxygen (O) were found. CH-Fe<sup>0</sup> displayed an emission energy at 6.9 keV in the resultant spectrum indicated the reduction of Fe ions to elemental Fe.

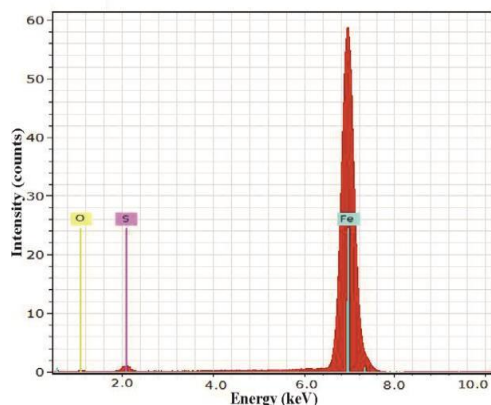


**Fig. 5:** Energy dispersive spectrum of Ch-Fe<sup>0</sup> nanoparticles

Earlier researcher (Madhavi et al 2014) reported that the EDS analysis of the CMC stabilized Fe<sup>0</sup> nanoparticles reveals a strong signal for iron at 6.4 keV, characteristic of iron metal. The energy dispersive spectrograph reveals a strong signal in the iron region (6.9 keV) confirms the formation of iron nanoparticles. Similarly, earlier studies (Weng et al 2013) observed the presence of strong signal in the iron region. In the EDS spectrum of CH-Fe<sup>0</sup>, iron was the major portion (73.01% in mass), while the remaining weaker elemental signals for sulfur (16.13% in mass) and oxygen (10.86% in mass) were also obtained. The weaker signals recorded in the EDS spectrum were possibly due to the elements from precursor salts used during nanoparticles synthesis.

### 3.2.5. Atomic Force Microscopy

The size, shape, morphology, and distribution of chitosan stabilized zerovalent iron nanoparticles in atomic force microscopy predominantly assured the homogeneity and the respective size. The observed particles exhibited spherical in shape and showed aggregation (Fig. 6). Earlier researcher (Prema et al 2017) reported that of CMC stabilized silver nanoparticles was spherical in shape and also indicated that the particles were well separated showing no agglomeration in the two dimensional micrograph. The 3D image of the stabilized nanoparticles showed sharp peaks with lower to higher sizes of the nanoparticles. The size and shape of the nanoparticles depends on the concentration and type of reducing as well as stabilizing agents used in the synthesis (Sharma et al 2009).

### 3.2.6. Particle size and Zeta potential study of chitosan stabilized iron nanoparticle

The study was conducted to determine the size distribution of nanoparticles as well as to measure zeta potential of synthesized chitosan stabilized iron nanoparticles. The z-average of CH-Fe<sup>0</sup> was found to be 44.7 nm (Fig. 7). It showed the average particle diameter was 64.8 nm and the polydispersity index (PDI) was 1.062. The zeta potential of the synthesized chitosan stabilized iron nanoparticle was highly negative and it was found to be -47 mV (Fig. 8). It mainly focuses the stability behavior of the synthesized Ch-Fe<sup>0</sup> nanoparticles which showed good stability. The negative charge in zeta potential indicated that the particle size is smaller than 100nm.

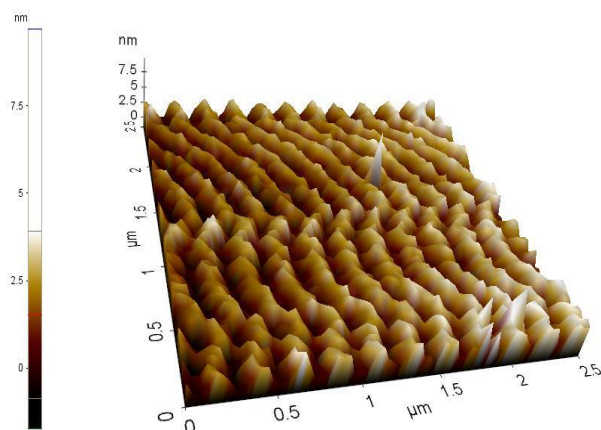


**Fig. 6:** Three dimensional images of chitosan stabilized zerovalent iron nanoparticles

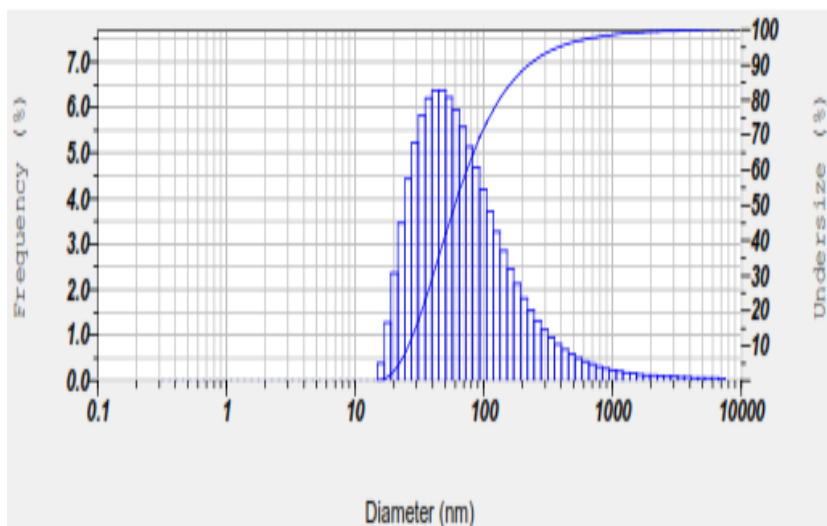


**Fig. 7:** Particle size distribution study of synthesized chitosan stabilized iron nanoparticle

In contradictory to the previous report, the zeta potential of the synthesized nanoparticle was found to be negative and the particle size was also found to be lesser than 100nm while chitosan was used as stabilizing agent. Similarly, earlier studies (Singh et al 2015) reported that the dynamic light scattering particle size analysis results indicated the hydrodynamic diameter of the particles size range was 50–150 nm with a 0.191 polydispersity index and the average particle size was 97 nm. Likewise, earlier scientist (Otari et al 2012) pointed out that the cluster size distribution of AgNPs was around 100nm measured by Dynamic Light Scattering (DLS).

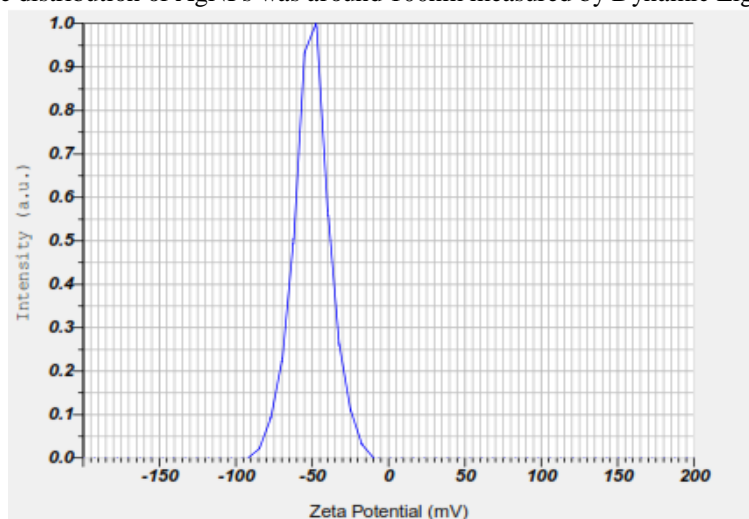


**Fig. 8:** Zeta potential analysis of synthesized chitosan stabilized iron nanoparticle

#### 4. CONCLUSIONS

Based on the obtained results, it can be concluded that RSM is one of the most useful methods to optimize the experimental conditions of different parameters in the reaction medium to develop a high yield of Chitosan stabilized ZVINPs synthesizing techniques. Subsequently, the DOE employed FCCCD under RSM was used for the complex process optimization of four important parameters. The smallest particle size (44nm) was obtained at the optimized synthesis conditions of precursor salt  $\text{FeSO}_4$  concentration 0.1 Molar, reducing agent  $\text{KBH}_4$  3ml,  $\text{N}_2$  gas purging time 30 minutes, stabilizing agent chitosan at 0.5% concentration and it is believed that these parameters are highly suitable for in bulk production of spherical chitosan stabilized zerovalent iron nanoparticles with diameter of 44–124 nm.

#### ACKNOWLEDGEMENTS

The authors are very grateful to V.H.N.Senthikumara Nadar College Managing Board, Virudhunagar for providing facilities and Alagappa University, CECRI, Karaikudi for technical assistance.

#### CONFLICT OF INTEREST

The author declares that they have no conflicts of interest

## REFERENCES

- [1] Zhang W.X. 2003. Nanoscale iron particles for environmental remediation: An Overview. *Journal of Nanoparticle Research*, 5: 323–332.
- [2] He F. and Zhao D. Y. 2005. Preparation and characterization of a new class of starch-stabilized bimetallic nanoparticles for degradation of chlorinated hydrocarbons in water. *Environmental Science and Technology*, 39(9):3314–3320.
- [3] Adewuyi S., Sanyaolu N. O., Amolegbe S. A., Sobola A. O. and Folarin O. M. 2012. Poly [ $\beta$ -1 $\rightarrow$ 4-2-amino-2-deoxy-D-ghicopyranose] based zero valent nickel nanocomposite for efficient reduction of nitrate in water. *Journal of Environmental Sciences*, 24(9):1702–1708.
- [4] Akinremi C. A., Oyelude V. B., Adewuyi S., Amolegbe S. A. and Arowolo T. 2013. Reduction of bromate in water using zerovalent cobalt 2,6-pyridine dicarboxylic acid crosslinked chitosan nanocomposite. *Journal of Macromolecular Science Part A*, 50(4): 435–440.
- [5] Geng B., Jin Z.H., Li T.L. and Qi X.H. 2009b. Kinetics of hexavalent chromium removal from water by chitosan-Fe<sup>0</sup> nanoparticles. *Chemosphere*, 75(6): 825-830.
- [6] Reddy L.V., Wee Y.J. and Yun J.S. 2008. Optimization of alkaline protease production by batch culture of *Bacillus* sp. RKY3 through Plackett–Burman and response surface methodological approaches. *Bioresource Technology*, 99(7): 2242-2249.
- [7] Liang Y.Y. and Zhang L.M. 2007. Bioconjugation of papain on superparamagnetic nanoparticles decorated with carboxymethylated chitosan. *Biomacromolecules*, 8(5):1480-1486.
- [8] Geng B., Jin Z.H., Li T.L. and Qi X.H. 2009a. Preparation of chitosan-stabilized Fe<sup>0</sup> nanoparticles for removal of hexavalent chromium in water. *Science of the Total Environment*, 407(18): 4994-5000.
- [9] Bhatia S.C. and Ravi N. 2000. A magnetic study of a Fe-chitosan complex and its relevance to other biomolecules. *Biomacromolecules*, 1(3): 413-417.
- [10] Bhatia S.C. and Ravi N. 2003. A Mossbauer study of the interaction of chitosan and D-glucosamine with iron and its relevance to other metalloenzymes. *Biomacromolecules*, 4(3): 723-727.
- [11] Sun Y.P., Li X.Q., Cao J., Zhang W.X. and Wang H.P. 2006. Characterization of zero-valent iron nanoparticles. *Advances in Colloid Interface Science*, 120(1-3): 47-56.
- [12] Singhal R.K., Gangadhar B., Basu H., Manisha V., Naidu G.R.K. and Reddy A.V.R. 2012. Remediation of malathion contaminated soil using zero valent iron nano-particles. *American Journal of Analytical Chemistry*, 3(1): 76-82.
- [13] Madhavi V., Prasad T.N.V.K.V., Ravindra Reddy B., Bhaskar Reddy A.V. and Gajulapalle, M. 2014. Conjunctive effect of CMC-zero-valent iron nanoparticles and FYM in the remediation of chromium-contaminated soils. *Applied Nanoscience*, 4(4): 477-484.
- [14] Xu C.H., Zhu L.J., Wang X.H., Lin S. and Chen Y.M. 2014. Fast and high efficient removal of chromium from aqueous solution using nanoscale zerovalent iron/activated carbon (NZVI/AC). *Water Air and Soil Pollution*, 225(2): 1845-1857.
- [15] Manning B.A., Kiser J. R., Kwon H. and Kanel S. R. 2007. Spectroscopic investigation of Cr(III) and Cr(VI)-treated nanoscale zerovalent iron. *Environmental Science and Technology*, 41(2): 586-592.
- [16] Alidokht L., Khataee A.R., Reyhanitabar A. and Oustan S. 2011. Reductive removal of Cr(VI) by starch-stabilized Fe<sup>0</sup> nanoparticles in aqueous solution. *Desalination*, 270 (1-3): 105-110.
- [17] Weng X., Lin S., Zhong Y. and Chen Z. 2013. Chitosan stabilized bimetallic Fe/Ni nanoparticles used to remove mixed contaminants-amoxicillin and Cd(II) from aqueous solutions. *Chemical Engineering Journal*, 229: 27-34.
- [18] Prema P., Thangapandiyar S. and Immanuel G.: CMC stabilized nano silver synthesis, characterization and its antibacterial and synergistic effect with broad spectrum antibiotics. *Carbohydrate Polymers*, 158: 141-148.
- [19] Sharma V.K., Yngard R.A. and Lin Y. 2009. Silver nanoparticles: green synthesis and their antimicrobial activities? *Advances in Colloids and Interface Science*, 145 (1):83-96.
- [20] Singh P., Kim Y.J., Singh H., Wang C., Hwang K.H., Farh M.E.A. and Yang D.C. 2015. Biosynthesis, Characterization and antimicrobial application of silver nanoparticles. *International Journal of Nanomedicine*, 10: 2567-2577.
- [21] Otari S.V., Patil R.M., Nadaf N.H., Ghosh S.J. and Pawar S.H. 2012. Green biosynthesis of silver nanoparticles from an actinobacteria *Rhodococcus* sp. *Materials Letters*, 72: 92–94.